Synthesis and characterization of new palladium (II) and silver (I) thiosemicarbazone derived by acenaphthenequinone complexes and their antimicrobial activity

Ashraf A. Aly [a,*], Elham M. Abdallah [a], Salwa A. Ahmed [a], Mai M. Rabee [a], Olaf Fuhr [b], Mahmoud A.A. Ibrahim [a,c], Hayat Ali Alzahrani [d], Bahaa G.M. Youssif [e,*]

[a] *Chemistry Department, Faculty of Science, Minia University, 61519 El-Minia, Egypt*
[b] *Institute of Nanotechnology (INT) and Karlsruhe Nano Micro Facility (KNMFi), Karlsruhe Institute of Technology (KIT), Hermann-von-Helmholtz-Platz 1, 76344 Eggenstein-Leopoldshafen, Germany*
[c] *School of Health Sciences, University of KwaZulu-Natal, Westville Campus, Durban 4000, South Africa*
[d] *Applied Medical Science College, Medical Laboratory Technology Department, Northern Border University, Arar, KSA*
[e] *Department of Pharmaceutical Organic Chemistry, Faculty of Pharmacy, Assiut University, Assiut, Egypt*

Keywords:
Pd complexes
Ag complexes
X-ray structure
Antimicrobial
Topoisomerase IV Inhibitors

A B S T R A C T

The ability of substituted acenaphthenequinone-thiosemicarbazones to do complexation with Pd(II) and Ag(I) salts was investigated. The obtained Pd(II) **5a-f** and Ag(I) **7a-f** complexes showed that ligation was occurred during the reaction of two equivalents of the ligands with one equivalent of the metal salts. In case of Pd complexes **5a-f**, two moles of HCl were eliminated during complexation process. Whereas direct ligation was occurred during complexation of one mole of $AgNO_3$ and two moles of ligands to form the corresponding cationic-anionic salts **7a-f**. IR, NMR, and UV–vis spectra were used to deduce the structure of the formed metal complexes. X-ray structure analysis proved the *syn*-form of bis(bidentate) structure of Pd complex **5e**, as Pd showed a square planar coordination with two sulfur and two nitrogen atoms. The cationic-anionic nature of silver complexes was revealed by molar conductance. UV–visible spectra were also investigated by means of Time-Dependent Density-Functional Theory (TD-DFT) computations. The obtained metal complexes were also investigated asantibacterial and antifungal agents. Compounds **5f**, **5e**, **7d**, and **7f** were found to be the most active and effective against the four bacterial strains, with compound **7f** having the most potent action. Compound **7f** (R 3-OMe-Ph) showed MIC values of 0.066, 0.018, 0.018, and 0.033 μg/mL against *B. subtilis, S. aureus*, *E. coli,* and *K. pneumoniae*, respectively. For compound **7d** (R Benzyl), the MIC values are found as 0.028, 0.057, 0.028, and 0.028 μg/mL against the same previous bacterial strains. Compounds **5d**, **5e**, **7c**, and **7f** demonstrated promising antifungal activity against *C. albicans* with MIC values of 0.029, 0.023, 0.018, and 0.027 μg/ml, respectively, when compared to the reference **fluconazole**, which had a MIC value of 0.020 μg/ml. Compound **7f** revealed inhibitory activity of *E. coli* DNA gyrase (IC_{50} 210 ± 15 nM, respectively) being 1.2-folds less potent than the reference **novobiocin** (IC_{50} 170 ± 20 nM).

1. Introduction

Thiosemicarbazones have a wide range of pharmacological characteristics, particularly as antiphrastic [1], antibacterial [2], antioxidant [3], and anticancer agents [4]. Moreover, thiosemicarbazone derivatives and their metal complexes have generated significant attention in chemistry and biology [5]. It was reported that acenaphthenequinone thiosemicarbazone reacted with various metal complexes and the formed complexes showed high anticancer efficacy [5]. Meanwhile, acenaphthenequinone thiosemicarbazones have piqued the interest of researchers due to the discovery of their unusual biological activity, such as antibacterial [6] and anti-HIV, anticancer [7].

* Corresponding authors.
E-mail addresses: ashrafaly63@yahoo.com (A.A. Aly), drelham2007@yahoo.com (E.M. Abdallah), salwa_kasem2003@yahoo.com (S.A. Ahmed), meemoo8791@yahoo.com (M.M. Rabee), olaf.fuhr@kit.edu (O. Fuhr), m.ibrahim@compchem.net (M.A.A. Ibrahim), Dr.hayatalzahrani@hotmail.com (H. Ali Alzahrani), bgyoussif2@gmail.com (B.G.M. Youssif).

Previously it was reported that the coordination of geometry around Pd in Pd-thiosemicarbazone complex **I** (Fig. 1) was as a square planner form [8]. Differently, the structure of palladium(II) complexes of 5-substituted isatin thiosemicarbazones **II** formed *via* the coordination of N and O atoms. In comparison, the third bond in **II** was formed *via the* elimination of an HCl molecule from the proton of the thiol group with one chlorine of $PdCl_2$ (Fig. 1) [9]. In Pd-thiosemicarbazone **III**, the Pd(II) ions adopted a distorted square planar geometry, where the Pd atom was bonded to monobasic tetradentate ONS donor molecules, and the fourth vacant site was occupied by triphenylphosphine ligand (Fig. 1) [10]. Another type of Pd-thiosemicarbazone complex **IV** of the general formula $Pd\{CpFe(\eta^5\text{-}C_5H_4CH{=}N{-}N{=}C(S)NH_2\}_2$ was synthesized with formylferrocene thiosemicarbazone as a two bidentate ligands (Fig. 1) [11]. In the latter, Pd also showed a square planar geometry with a Pd (II) center and two bidentate ligands, each of which coordinates to Pd(II) *via* the imine nitrogen atom and the thioamide sulfur atom of the deprotonated ferrocenyl thiosemicarbazone ligand (Fig. 1) [11]. In the case of Ag(I)-thiosemicarbazone **V** (Fig. 1), the bond angles around the silver(I) ions are in the range of ca. 71.87(8)–123.91(7)°, corresponding to strongly distorted tetrahedral geometry and the distortion of the tetrahedral geometry is caused by the bulky PPh_3 ligands [12]. Mixed Ag complex **VI** was synthesized by reacting $AgNO_3$, 1,10-phenanthroline (phen), and 2-formylpyridine-N(4)-R-thiosemicarbazone in a 1:1:1 M ratio, respectively (Fig. 1) [13].

Palladium [Pd(II)] organometallic complexes with thiosemicarbazone ligands have sparked interest due to the stability of the formed complex [14]. Pd(II) complexes are the most appealing candidates among transition metal complexes, making them a good alternative for metal-based drugs[15–17]. Thirty-four thiosemicarbazones and *S*-alkyl thiosemicarbazones, and some of their Pd(II) complexes were obtained to investigate antimicrobial activity. MIC values of the compounds were determined against *Escherichia coli, Klebsiella pneumoniae, Proteus mirabilis, Pseudomonas aeruginosa, Salmonella typhi, Shigella flexneri, Staphylococcus aureus, S. epidermidis*, and *Candida albicans* [18]. Pd-complexes showed moderate antimicrobial activity compared with their free ligands [18]. Another types of metal complexes, prepared from the reaction of steroidal thiosemicarbazone with $[Pd(DMSO)_{(2)}Cl_{(2)}]$ [19]. The results of antibacterial activity showed that steroidal complexes are better inhibit growth as compared to steroidal thiosemicarbazones of both types of the bacteria (gram-positive and gram-negative); compared to **amoxicillin** [19].

Chelation, in particular, is a well-known technique for modifying the physicochemical properties of silver compounds and including biologically active ligands on their own [20–24]. Density functional theory and UV–Vis studies of some Ag(I) complexes have shown distorted tetrahedral geometry around the silver(I) ion [25]. Silver was proposed to act by binding to key functional groups of enzymes [26]. Silver ions cause the release of K^+ ions from bacteria; thus, the bacterial plasma or cytoplasmic membrane, which is associated with many important enzymes, is an important target site for silver ions [26]. In addition to their effects on bacterial enzymes, silver ions caused marked inhibition of bacterial growth and were deposited in the vacuole and cell wall as granules [27].

DNA gyrase and topoisomerase IV (Topo IV) are type IIa topoisomerases found in bacteria that play important roles in regulating the topological state of DNA during transcription and replication [28]. At the end of the replication process, Topo IV is primarily responsible for decatenation, while DNA gyrase is critical for DNA replication initiation, new DNA elongation, and negative supercoiling during replication [29].

We previously investigated the ability of substituted thiocarbohydrazones to complex with Cu(I), Co(II), and Ni(II) salts [30]. To obtain reliable results for the experimental values, theoretical calculations were performed at the B3LYP level with the 6–31 + G(d) and LANL2DZ basis sets [30]. Moreover, Aly *et al.* [31] also reported on the synthesis of paracyclophane-substituted thiosemicarbazones, thiocarbazones, hydrazones, and thioureas to investigate their complexation capability towards Cu(I) and Cu(II) salts. The paracyclophane-substituted ligands were found to be tris(bidentate) and bis(bidentate) [31].

An interesting series of four complexes of acenaphthoquinone 3-(4-benzylpiperidyl)thiosemicarbazones were previously prepared [32]. As, cobalt metal was linked by deprotonated thiosemicarbazone ligands

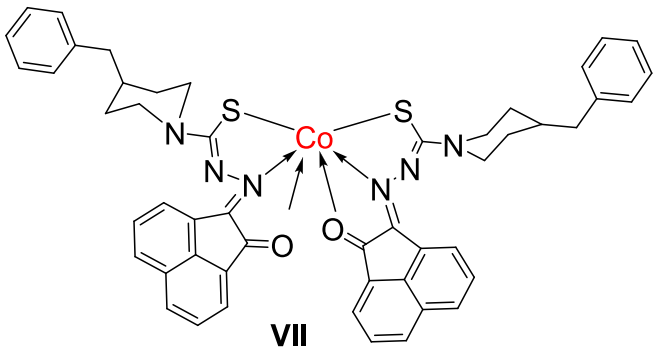

Fig. 2. Structure of acenaphthoquinone 3-(4-benzylpiperidyl)thiosemicarbazone-Co complex (VII).

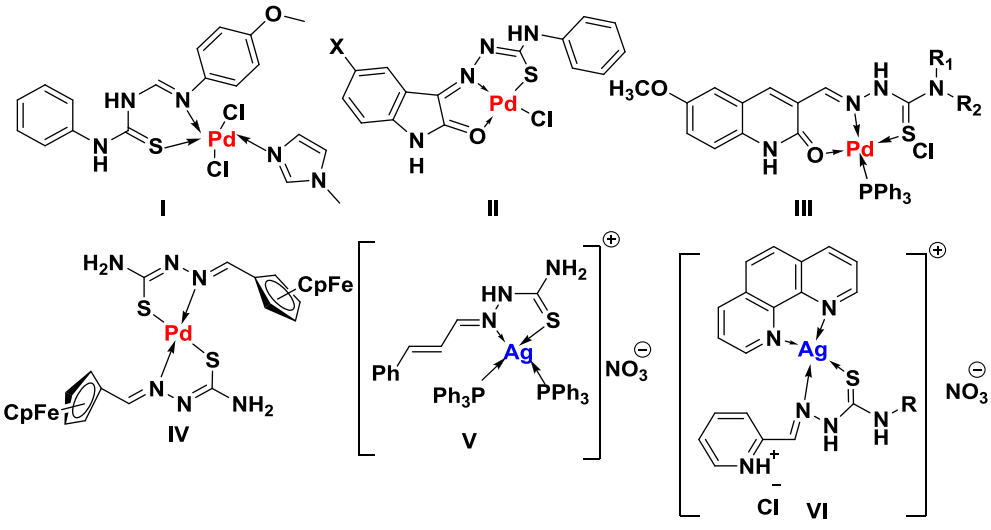

Fig. 1. Structures of various Pd(II)- and Ag(I)-thiosemicarbazones complexes.

using S-donor atoms and coordinated with the same ligands with both N- and O-heteroatoms in a meridional fashion (**VII**, Fig. 2) [32]. Antibacterial activity of the ligand and complexes were screened against two-gram negative bacteria *Escherichia coli*, *Pseudomonas aeruginosa* and two-gram positive bacteria *Staphylococcus aureus* and *Bacillus subtilis*. The electron micrograph images display damage to microbial cell wall upon treatment with the compounds [32].

Ciprofloxacin is one of a new generation of fluorinated quinolones structurally related to nalidixic acid. The primary mechanism of action of ciprofloxacin is inhibition of bacterial DNA gyrase [33]. **Fluconazole** has still known as the most important drug for treatment of the systemic fungal infections [34]. **Novobiocin**, is also known as **albamycin** or **cathomycin**, is an aminocoumarin antibiotic that is produced by the actinomycete *Streptomyces niveus*, which has been identified as a subjective synonym for *S. spheroides* a member of the class *Actinomycetia* [35].

Based upon those mentioned above, it was found interesting to investigate the structure and geometry of metal-formed Pd(II) and Ag(I) complexes from the reaction of acenonaphthoquinone-thiosemicarbazones with $PdCl_2$ and $AgNO_3$ (Fig. 3). The newly synthesized complexes **5a-f** and **7a-f** were tested for their antibacterial activity against two Gram-positive bacteria, *Staphylococcus aureus* and *Bacillus subtilis*, two Gram-negative bacteria, *Escherichia coli* and *Klebsiella pneumoniae*, and antifungal activity against two fungi, *Candida albicans,* and *Aspergillus niger*. The most potent complexes will be tested against *E. coli* DNA gyrase and topoisomerase IV as potential targets for antibacterial activity.

2. Experimental

2.1. Chemistry

Compounds **3a-f** were prepared according to previously reported procedures [36–38].

2.1.1. Preparation of ligands; synthesis of substituted hydrazinecarbothioamides *3a-f*

Compounds **3a**–**f** were synthesized by refluxing solutions of acenaphthenequinone **1** (1.82 g, 10 mmol) in absolute EtOH (100 mL) containing triethylamine (0.5 mL) and different solutions of thiosemicarbazide derivatives **2a**–**f** for 5–10 h. After precipitation with ethanol, the products were left to stand and then collected by filtration. The resulting solid was recrystallized from the stated solvents to give yellow to orange crystals.

2.1.2. General procedure for synthesis of complexes 5a-f and *7a-f*

A mixture of two mmol of **3a-f** with one mmol of either Pd(II) chloride or $AgNO_3$ in 20 mL EtOH was stirred at room temperature (the reaction was followed up by TLC till the consummation of the starting ligand). The formed precipitate of either **5a-f** or **7a-f** was filtered off and washed with H_2O (100 mL), followed by 50 mL EtOH. Physical and analytical data of the obtained products **5a-f** or **7a-f** were illustrated in Tables 1-4.

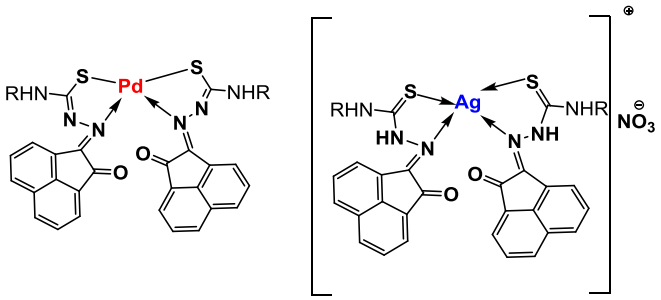

Fig. 3. Structure of target complexes 5a-f and 7a-f.

2.2. Biology

2.2.1. Determination of minimum inhibitory concentration (MIC)

Using the serial dilution method, all the synthesized compounds were tested for their ability to inhibit the growth of two Gram-positive bacteria, *Staphylococcus aureus* and *Bacillus subtilis*, two Gram-negative bacteria, *Escherichia coli* and *Klebsiella pneumoniae*, and two fungi, *Candida albicans,* and *Aspergillus niger* [39,40]. See Appendix A (Supplementary File).

2.2.2. Determination of inhibitory activities on e. Coli and S. Aureus DNA gyrase and topoisomerase IV

All the final compounds were tested for *E. coli* DNA gyrase inhibitory activity in a supercoiling assay [28,29]. See Appendix A (Supplementary File).

2.3. X-ray structure analysis

2.3.1. X-ray structure determination of *5e*

Single crystal X-ray diffraction data of **5e** were collected on a StadiVari diffractometer with monochromated Mo Kα (0.71073 Å) radiation at 180 K. Using Olex2 [41], the structures were solved with the ShelXT [42] structure solution program using Intrinsic Phasing and refined with the ShelXL [43] refinement package using Least Squares minimization. Refinement was performed with anisotropic temperature factors for all non-hydrogen atoms; hydrogen atoms were calculated on idealized positions. Structural data and refinement details are summarized in SI Table 1.

Crystallographic data for compounds **5e** reported in this paper have been deposited with the Cambridge Crystallographic Data Centre as Supplementary Information no. CCDC-2268761. Copies of the data can be obtained free of charge from https://www.ccdc.cam.ac.uk/structures/.

2.4. DFT and TD-DFT calculations

Geometry optimizations were carried out on the molecular structure of the Pd(II) and Ag(I) complexes (**5e** and **7e**, respectively), in the presence of dichloromethane solvent at the B3LYP/6–31 + G* level of theory for all atoms except the Pd and Ag that were treated with B3LYP/LANL2DZ basis set. Furthermore, the Time-dependent (TD)-DFT computations were performed employing the PBE0 method together with the same adopted basis sets. All the abovementioned calculations were established with the aid of Gaussian09 software [44].

Table 1
Physical data and yield in g (%) of complexes **5a-f** and **7a-f.**

Complex	Color	m.p (°C)	Yield (g, %)
5a	Brown	> 360	0.23 g (78)
5b	dark red	> 360	0. 14 g (80)
5c	red	338–340 (decomp)	0.14 g (60)
5d	Red	328–330 (decomp)	0.17 g (64)
5e	Red	> 360	0.17 g (75)
5f	Red	342–344 (decomp)	0.20 g (55)
7a	Orange	> 360	0.14 g (89)
7b	Orange	> 360	0.40 g (80)
7c	Orange	322–324 (decomp.)	0.10 g (70)
7d	Orange	330–332 (decomp.)	0.17 g (75)
7e	Orange	320–322 (decomp.)	0.28 g (80)
7f	Orange	>360	0.23 g (83)

Table 2
Stoichiometric formation and analytical data of metal complexes of Pd (II) **5a-f**, and Ag(I) **7a-f.**

Ligand	Metal salt	Complex	Stoichiometry	Molecular formula	C, ; H, Cl, ; N, ; S,
3a	$PdCl_2$	**5a**	2:1	$C_{28}H_{20}N_6O_2PdS_2$	Calcd: C, 52.30; H, 3.14; N, 13.07; S,9.97 Found: C, 52.32; H, 3.16; N, 13.09; S, 9.95
3b	$PdCl_2$	**5b**	2:1	$C_{32}H_{24}N_6O_2PdS_2$	Calcd: C, 55.29; H, 3.48; N, 12.09; S, 9.22 Found: C, 55.27; H, 3.15; N, 12.07; S, 9.20
3c	$PdCl_2$	**5c**	2:1	$C_{38}H_{36}N_6O_2PdS$	Calcd: C, 58.57; H, 4.66; N, 10.78; S, 8.23 Found: C, 58.55; H, 4.68; N, 10.76; S,8.24
3d	$PdCl_2$	**5d**	2:1	$C_{40}H_{28}N_6O_2PdS$	Calcd: C, 60.41; H, 3.55; N, 10.57; S, 8.06 Found: C, 60.43; H, 3.53; N, 10.55; S, 8.04
3e	$PdCl_2$	**5e**	2:1	$C_{38}H_{24}N_6O_2PdS_2$	Calcd: C, 59.49; H, 3.43; N, 10.95; S, 8.36 Found: C, 59.47; H, 3.41; N, 10.93; S, 8.34
3f	$PdCl_2$	**5f**	2:1	$C_{40}H_{28}N_6O_4PdS_2$	Calcd: C, 58.08; H, 3.41; N, 10.16; S, 7.75 Found: C, 58.06; H, 3.43; N, 10.18; S, 7.77
3a	$AgNO_3$	**7a**	2:1	$C_{28}H_{22}AgN_7O_5S_2$	Calcd: C, 47.47; H, 3.13; N, 13.84; S, 9.05 Found: C, 47.16; H, 3.15; N, 13.76; S, 9.07
3b	$AgNO_3$	**7b**	2:1	$C_{32}H_{26}AgN_7O_5S_2$	Calcd: C, 50.53; H, 3.45; N, 12.89; S, 8.43 Found: C, 50.46; H, 3.62; N, 12.75; S, 8.33
3c	$AgNO_3$	**7c**	2:1	$C_{38}H_{38}AgN_7O_5S_2$	Calcd: C, 54.03; H, 4.53; N, 11.61; S, 7.59 Found: C, 54.12; H, 4.66; N, 11.74; S, 8.62
3d	$AgNO_3$	**7d**	2:1	$C_{40}H_{30}AgN_7O_5S_2$	Calcd: C, 55.82; H, 3.51; N, 11.39; S, 7.45 Found: C, 55.62; H, 3.52; N, 11.53; S, 7.33
3e	$AgNO_3$	**7e**	2:1	$C_{38}H_{26}AgN_7O_5S_2$	Calcd: C, 54.81; H, 3.15; N, 11.78; S, 7.70

(*continued on next page*)

Table 2 (*continued*)

3f	$AgNO_3$	**7f**	2:1	$C_{40}H30AgN_7O_7S_2$	Found: C, 54.96; H, 3.13; N, 11.91; S, 7.56 Calcd: C, 53.82; H, 3.39; N, 10.98; S, 7.18 Found: C, 53.96; H, 3.43; N, 11.12; S, 7.36

Table 3
Chemical shifts (δ), including ^{1}H spectroscopic data for ligands **3d** and its complexes in **5d** and **7d.**

No	Compd.	^{1}H NMR (δ,DMSO-d_6)
1	**3d**	δ_H 12.70 (s, 1H, NH), 9.94 (bs 1H, NH), 8.37 (d, J = 8.2; 1H), 8.16 (d, J = 8.3; 1H), 8.10 (d, J = 7.0; 1H), 8.00 (d, J = 7.0; 1H), 7.88 (dd, J = 8.0, 7.2; 1H); 7.83 (dd, J = 8.2, 7.2; 1H), 7.42 (d, J = 7.2; 2H), 7.37 (dd, J = 7.7, 7.3; 2H), 7.28 (t, J = 7.1; 1H), 4.94 (d, J = 6.2; 2H)
2	**5d**	δ_H 10.00 (bs; 1H, NH), 8.65 (d, J = 8.2; 1H), 8.10 (d, J = 8.3; 1H), 8.10 (d, J = 7.0; 1H), 8.00 (d, J = 7.0; 1H), 7.80 (dd, J = 8.0, 7.2; 1H); 7.75 (dd, J = 8.2, 7.2; 1H), 7.38 (d, J = 7.2; 2H), 7.30 (dd, J = 7.7, 7.3; 2H), 7.20 (t, J = 7.1; 1H), 4.90 (d, J = 6.2; 2H)
3	**7d**	δ_H 10.10 (bs; 1H, NH), 8.37 (d, J = 8.2; 1H), 8.30 (d, J = 8.3; 1H), 8.20 (d, J = 7.0; 1H), 8.12 (d, J = 7.0; 1H), 7.78 (dd, J = 8.0, 7.2; 1H); 7.70 (dd, J = 8.2, 7.2; 1H), 7.30 (d, J = 7.2; 2H), 7.35 (dd, J = 7.7, 7.3; 2H), 7.22 (t, J = 7.3; 1H), 4.80 (d, J = 6.2; 2H),

3. Results and discussion

3.1. Chemistry

The strategy of preparation of acenonaphthoquinone-thiosemicarbazone ligands **3a-f** [36–38], bis(bidentate) Pd-thiosemicarbazone complexes **5a-f** is outlined in Scheme 1. First, two equivalents of acenonaphthoquinone (**1**) and one equivalent of thiosemicarbazides **2a-f** were allowed to react for 5–10 h in refluxing EtOH to give the corresponding ligands **3a-f** in 60–84 % yields. The bis (bidentate) Pd-complexes **5a-f** were obtained in good yields by reacting two equivalents of **3a-f** with one equivalent of $PdCl_2$ (**4**) in EtOH with stirring at room temperature for 12–18 h, the reaction proceeded to give the Pd-complexes **5a-f** in 55–80 % yield.

When, one equivalent of $AgNO_3$ (**6**) was added to two equivalents of **3a-f** in ethanol, Ag complexes **7a-f** were formed in 70–89 % yields (Scheme 2).

3.1.1. Characterization by mass spectroscopy and elemental analyses

The physical data and yield in g (%) of complexes **5a-f** and **7a-f** are as shown in Table 1. The molecular formulae of the obtained complexes were proved according to the mass spectroscopic data and the elemental analyses.

Table 2 illustrates the stoichiometric formation and analytical data of bis(bidentate) complexes of both Pd(II) **5a-f** and Ag(I) **7a-f**. The complexation was proved exact positive masses of ligands and the formed simulated metal complex between **3a-f** with either $PdCl_2$ (**4**) or $AgNO_3$ (**6**) help to support and deduce the chemical formula of the obtained complexes. In the case of complex **5a**, the mass spectroscopy displayed the dimer's molecular peak at m/z = 643.0 (65 %). The exact molecular formula of **5a** was in good agreement with the molecular formula of $C_{28}H_{20}N_6O_2PdS_2$ indicating that ligation was accompanied by elimination of two moles of HCl. On the other site, mass spectroscopy of complex **7a** showed the molecular ion peak of the dimer complex at m/z = 645.0 for [$(M)^{\cdot+}$] (42 %). In addition, elemental analysis of **7a** indicated the molecular formula as $C_{28}H_{22}AgN_7O_5S_2$. That supported the chelation between one mole of $Ag(NO_3)$ and two moles of the ligand was occurred without elimination of two hydrogens.

Table 4
IR absorption bands (υ, cm^{-1}) of ligands **3a-f** and their complexes of Pd(II) and Ag(I) complexes.

Ligand	Absorption of functional groups (ν) in ligands (cm^{-1})	Metal Complex	Absorption of functional groups (ν) in complexes (cm^{-1})
3a	ν(str NH): 3294, ν(str C═N): 1600, ν (str C═S): 1045 s	**5a**	ν(str. NH):3218, ν(str C═N): 1572, 1025 s, ν (M N): 625, ν(Pd-S): 473.
3b	ν(str NH): 3315 ν(str C═N): 1600, ν (str C═S): 1045 s	**5b**	(str NH):3179, ν(str C═N): 1565, ν(M N): 654, ν(Pd-S): 471
3c	ν(str NH): 3294 ν(str C═N): 1600, ν(str C═S): 1045 s	**5c**	ν(NH):3222, ν(C═N): 1570; ν(Pd-N): 625, ν(M S): 450
3d	ν(str NH): 3314 ν(str C═N): 1607, ν(str C═S): 1023 s	**5d**	ν(NH):3222, ν(C═N): 1574, ν(Pd-N): 695, ν(M S): 470
3e	ν(str NH): 3320 ν(str C═N): 1599, ν(str C═S): 1045 s	**5e**	ν(str NH):3235, ν(str C═N): 1573, ν(M N): 685, ν(Pd-S): 450
3f	ν(str NH): 3397, ν(str C═N): 1615, ν(str C═S): 1045 s	**5f**	ν(str NH):3276, ν(str C═N): 1574, ν(Pd-N): 679, ν(Pd-S): 470
3a	The same as above	**7a**	ν(str NH): 3210, ν(str C═N): 1570, ν (NO_3): 1384, ν(str C═S): 1024 s, ν(Ag-N): 650, ν(Ag-S): 471
3b	The same as above	**7b**	ν(str NH): 3222, ν(str C═N): 1590, ν(str C═S): 1030, ν(Ag-N): 650, ν(NO_3): 1384, ν(Ag-S): 490.
3c	The same as above	**7c**	ν(str. NH): 3374, ν(str C═N): 1503, ν(str C═S): 1018,ν(Ag-N): 550, (Ag-S): 472, ν(NO_3): 1384
3d	The same as above	**7d**	ν(str. NH): 3222, ν(str C═N): 1594, ν(str C═S): 1028 s, ν(Ag-N): 687, (Ag-S): 472, ν(NO_3): 1384
3e	The same as above	**7e**	ν(str. NH): 3235, ν(C═N): 1594, ν(str C═S): 1018 s, ν(Ag-N): 687, ν(Ag-S): 472, ν(NO_3): 1384
3f	The same as above	**7f**	ν(str NH): 3391, ν(str C═N): 1594, ν(str C═S): 1022 s, ν(Ag-N): 650, ν(NO_3): 1385, ν(Ag-S): 470.

3.1.2. Molar conductance

The molar conductance for the complexes for 10^{-3} M solutions of **7b** and **7f** in DMF and MeOH showed values ranging from 80.2 to 100.25 $S.cm^2.mol\ L^{-1}$ and values of 82.0 and 100.1 $S.cm^2.mol^{-1}$, respectively. The latter indicates an electrolyte type of 1:1 [45]. This is in agreement indicates if the molar conductance value is more than 30 $S.cm^2.mol\ L^{-1}$, the solution of the compound will have conductance activity [45]. Therefore, these types of complexes are electrolytic in solution.

3.1.3. Assignment of the Pd(II) and Ag(I) complexes by ^{1}H NMR spectra

There are remarkable chemical shifts (δ) in ^{1}H NMR spectra of compound **3d** compared with those in complexes **5d** and **7d** (Table 3). It was also observed that the hydrazono-NH signal disappeared in the spectra of complexes **5d** and **7d**. Accordingly, it can be deduced that

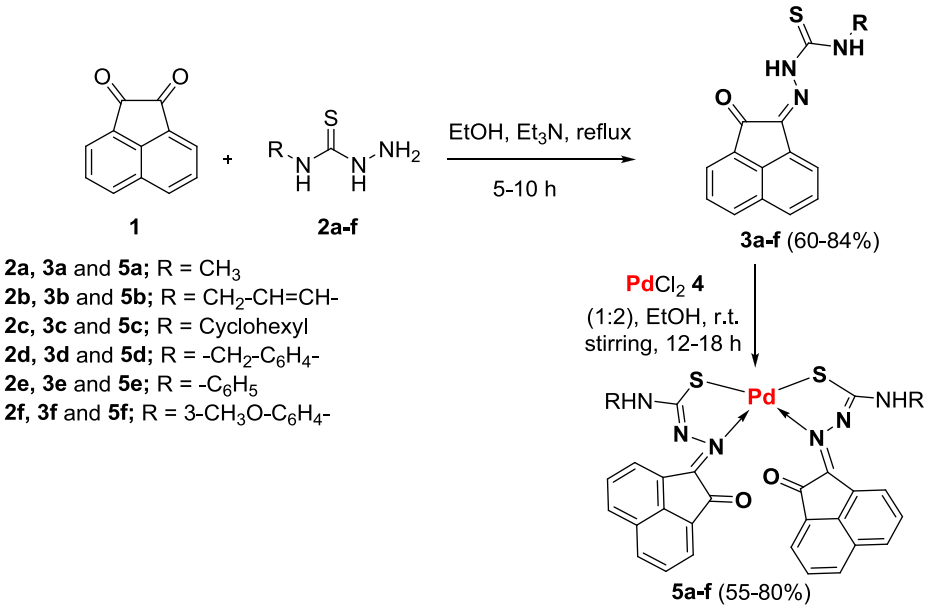

Scheme 1. Synthesis of ligands 3a-f and Pd-complexes 5a-f.

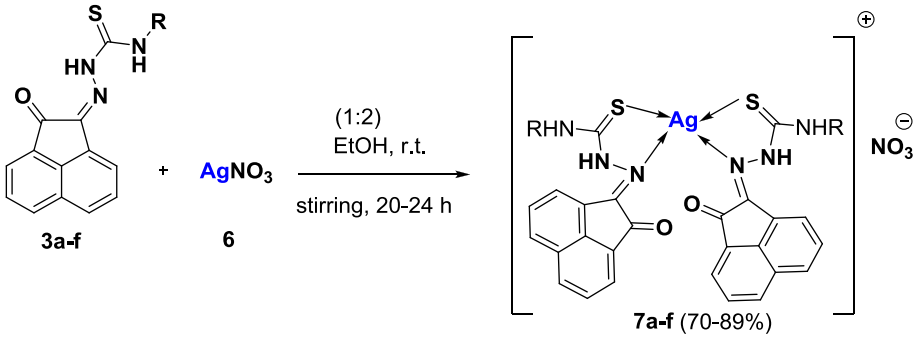

Scheme 2. Synthesis of Ag(I) complexes 7a-f.

chelation between $PdCl_2$ and $AgNO_3$ with ligands **3a-f** occurred *via* coordination between azomethine nitrogen and the central metal. Due to the low solubility of the obtained metal complexes, only two ^{1}H NMR spectra were measured and detected for compounds **5d** and **7d**.

3.1.4. Assignment by IR spectra

The significant bands in infrared spectra for thiosemicarbazones **3a-f** and Pd(II) and Ag(I) complexes are represented in Table 4. The symmetrical stretching NH_2 and NH bands for compounds **3a-f** were absorbed in the region at their expected region of IR spectra. The weak appearance of the NH groups in all metal complexes supported the chelation through the NH group and bond formation between M N. The absorption shifts of the functional groups NH and C═S from the ligands to the corresponding complexes confirmed that the chelating process indicates their coordination with the central metal. In **3c**, the absorption bands for NH and C═N appeared at υ = 3294 and 1600 cm ^{1}. The absence of the absorption of C═S indicated its conversion into thiol group. The center of coordination in **5c** was supported by the appearance of absorption bands at υ = 3222 and 1570 for NH and C═N groups. Besides that, new bands were appeared at υ = 625 and 450 cm ^{1} assigned to Pd-N and Pd-S groups. Thus, it can be deduced that Pd-complexation occurred between sulfur of thiol group and nitrogen heteroatoms. Moreover, elemental analysis of **5a** showed the chemical formula of **5a** as $C_{28}H_{20}N_6O_2PdS_2$ indicated a loss of one hydrogen atom from a molecule of **3a** was occurred during complexation process. Whereas, remarkable shift of C═N can be related to the change of electronic configuration of that group. Most indicative is the structure of the assigned complexes was supported depending upon the ^{1}H NMR spectra (Table 3) and revealed the removal of hydrogen from NH-2. From the above said, it can be deduced that complexation was occurred between Pd atom with sulfur and N heteroatoms. Since elemental analysis of **5a** indicated complexation between two moles of **3a** with $PdCl_2$ together with extrusion of two moles of HCl. Moreover, the IR spectrum of **7a** showed absorptions of NH, C═N and C═S, the proposed structure **7a** was as shown in Scheme 1. In **7b**, it is most indicative to observe bands at υ = Ag-S and Ag-N at 490 and 650 cm ^{1}, respectively. A sharp and strong band observed near 1380—1384 cm ^{1} in all Ag(I) complexes indicates the presence of the uncoordinated nitrate ion. In general, the IR spectra showed the most significant variations in the absorptions of the C═S and C═N groups, indicating that the coordination sites are with the nitrogen of the azomethine group and sulfur of C═S.

3.1.5. UV–vis studies

The UV–Visible spectra of some selected Pd- and Ag complexes are shown in Fig. 4 and were recorded from λ_{max} = 800 to 200 nm using dichloromethane as solvent at room temperature. Three absorption bands (i.e. compound **3d** showed λ_{max} = 250, 415 and 428 nm) with varying intensities can be observed in the ligands. The spectra of Pd(II) complex **5d** and **7d** showed three prominent bands. As Metal complex of

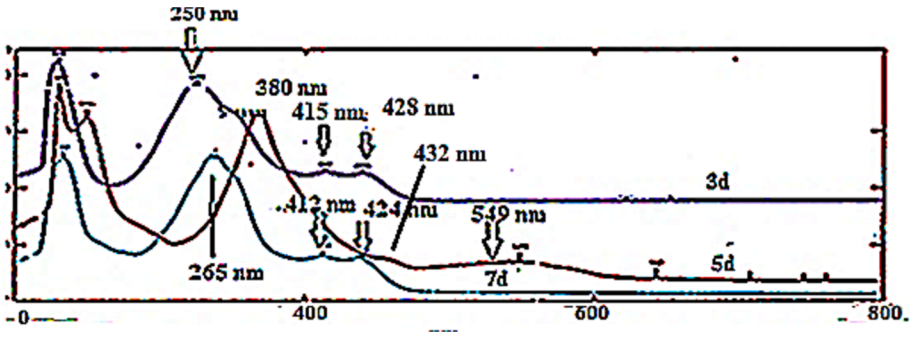

Fig. 4. Electronic absorption spectra of 3d and Pd(II) 5d and Ag(I) 7d complexes.

5d revealed three absorption bands at λ_{max} = 380, 432 and 549 nm, for two types of π-π* and one n-π* transitions, respectively. Whereas metal complex of **7d** showed bands λ_{max} = 265, 412 and 424 nm for one type of π-π* and n-π* transitions, respectively. In addition, the band at λ_{max} = 424–412 nm can be assigned to ligand-to-metal charge transfer (LMCT) transitions from sulfur to palladium ion.

Generally, the structure and the geometry of the obtained complexation between Pd salts and thiosemicarbazone moiety of 1:1 ratio was supported by those reported in the literature [16,17,46]. At the same time, the complexation between two moles of thiosemicarbazone derivatives and 1 mol of Pd salts and the direct formation of the structure was also supported with ref [47].

3.1.6. *X-ray structure analysis*

During recrystallization of **5e** from DMF, single crystals were obtained and X-ray structure analysis proved its structure as shown in Fig. 5. Compound **5e** crystallizes in the monoclinic space group *C2/c* with eight formula units per unit cell. Two molecules from two solvents were found in the crystal lattice; one announced to EtOH and other for DMF. These solvents are connected *via* hydrogen bonding to the main palladium complex with H···O interactions of 1.998 Å (H···O3) and 2.078 Å (H···O4). This complex consists of a palladium 2 + ion and two deprotonated thiosemicarbazone ligands. The palladium ion shows a square planar coordination with two sulfur and two nitrogen atoms with atomic distances of 2.258 Å for Pd–S bonds and 2.064 Å for Pd–N bonds. The sulfur and nitrogen donor atoms are arranged in *syn*-positions.

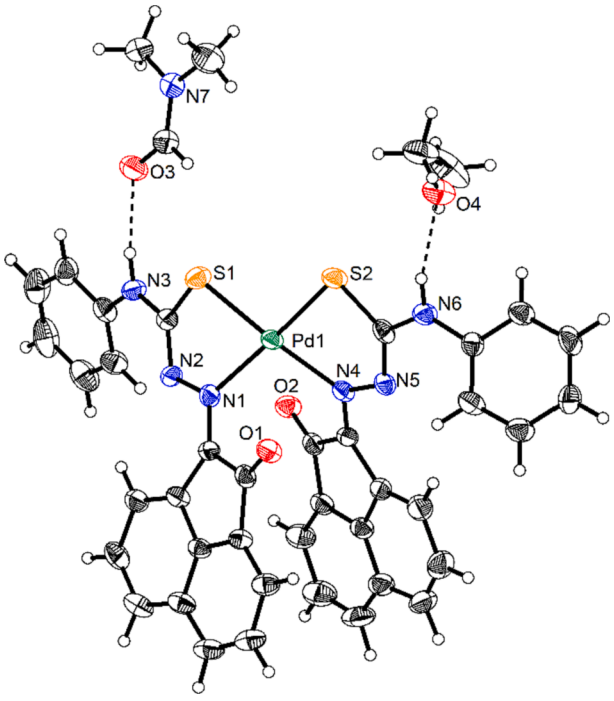

Fig. 5. Molecular structure of compound 5e as ORTEP plot (ellipsoids with 50% probability).

3.1.7. *DFT and TD-DFT calculations of complexes **5e** and **7e***

Using the density functional theory (DFT) calculations, molecular structures of the Pd(II) and Ag(I) complexes (**5e** and **7e**, respectively) were first optimized in the presence of dichloromethane solvent at the B3LYP functional, together with a basis set of 6–31 + G* for all atoms except the Pd and Ag that were treated with LANL2DZ basis set. The solvation model was implemented using the Polarizable Continuum Model (PCM). Time-dependent (TD)-DFT computations were then executed in a dichloromethane environment utilizing the PBE0 method with the incorporation of the abovementioned basis sets, in accordance with the earlier recommendations that confirmed its impressive alignment with the experimental outlines [48]. The optimized molecular structures of complexes **5e** and **7e**, along with their simulated UV–visible spectra, are illustrated in Fig. 6.

As evidenced in Fig. 6, the optimized structure of the selected Pd(II) complex **5e** was in observable agreement with the X-ray structural data displayed in Fig. 5. Apparently, slight differences between the structures of the complexes **5e**and **7e** were denoted, reflecting the influence of the central atom (i.e., Pd(II) and Ag(I)) on the distortion of the optimized geometry of the investigated complexes. For instance, the Pd–S and Ag–S bond lengths were observed with values of 2.33 Å and 2.64 Å, respectively. In line with experimental UV–visible spectra shown in Fig. 4, the simulated UV–visible spectra of Pd(II) and Ag(I) complexes (**5e** and **7e**, respectively), were detected with notable bands that assigned to π-π* and n-π* transitions, which were very similar to those displayed in Fig. 4.

From the above mentioned, it was deduced the followings:

(1) Elemental analyses and mass spectra confirmed the molecular formula of the assigned complexes. The isolated Pd(II) **5a-f** and Ag(I) **7a-f** complexes showed that ligation was occurred by reacting two equivalents of the ligands with one equivalent of the metal salts. In case of Pd-complexes two moles of HCl were eliminated. Whereas, Ag(I) complex acenaphthenequinone-thiosemicarbazones formed directly the cationic-anionic salts without elimination of any protons.
(2) IR and NMR spectra indicated the coordination active centers in the ligands that responsible for chelation. NMR spectra also confirmed the absence of hydrazine-NH.
(3) UV spectrum indicated absorption bands assigned to π-π* and n-π* transitions.
(4) Measurement of molar conductance of two examples of Ag-complexes **7a-f**, illustrates that the complex formed has a negative charge found out of the sphere and this negative charge is the nitrate anion.

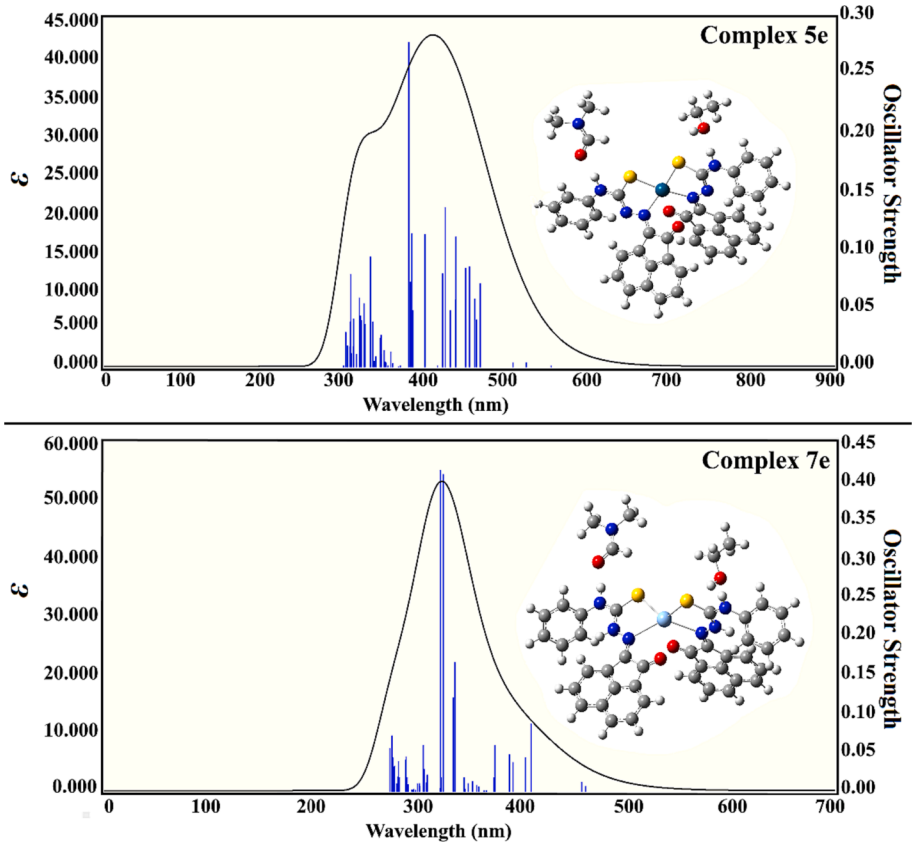

Fig. 6. Optimized molecular structures along with the UV–visible spectra of the Pd(II) and Ag(I) complexes (5e and 7e, respectively).

(5) X-ray structure analysis unambiguously proved the *syn*-structure and the geometry of the obtained complexes. However, it was expected that ligation would occur to give the *anti*- structure of the corresponding complexes (i.e. **5a-f**, Fig. 7).

3.2. Biology

3.2.1. Antibacterial activity

Using the serial dilution method, all the synthesized compounds were tested for their ability to inhibit the growth of two Gram-positive bacteria, *Staphylococcus aureus* and *Bacillus subtilis*, two Gram-negative bacteria, *Escherichia coli* and *Klebsiella pneumoniae*, and two fungi, *Candida albicans,* and *Aspergillus niger* [39,40]. **Ciprofloxacin** and **fluconazole** were used as controls against bacterial and fungal strains, respectively. Table 5 highlights the Minimum Inhibitory Concentration (MIC) values of synthesized compounds in μmol/mL and standard drugs. According to the data in Table 5 and Fig. 8, most of the tested compounds demonstrated moderate to good activity. Compounds **5e**, **5f**, **7d**, and **7f** were found to be the most active and effective against the four bacterial strains. Compound **7f** (R = 3-OMee-Ph) showed MIC values of 0.066, 0.018, 0.018, and 0.033 μg/mL against *B. subtilis, S. aureus*, *E. coli,* and *K. pneumoniae*, respectively. For compound **7d** (R = Benzyl) the MIC values are found as 0.028, 0.057, 0.028, and 0.028 μg/mL against the same previous bacterial strains. Against the same mentioned bacterial strains, compound **5e** (R = Ph) showed MIC values as 0.077, 0.035, 0.077, and 0.077 μg/mL. Whereas compound **5f** (R = 3-MeO-Ph) revealed MIC values of 0.039, 0.019, 0.039, and 0.019 μg/mL against *B. subtilis, S. aureus*, *E. coli,* and *K. pneumoniae*, respectively. Compound **7f** (R = 3-MeO-Ph) demonstrated comparable activity to the reference ciprofloxacin against *S. aureus* and *E. coli*, with MIC values of 0.018 and

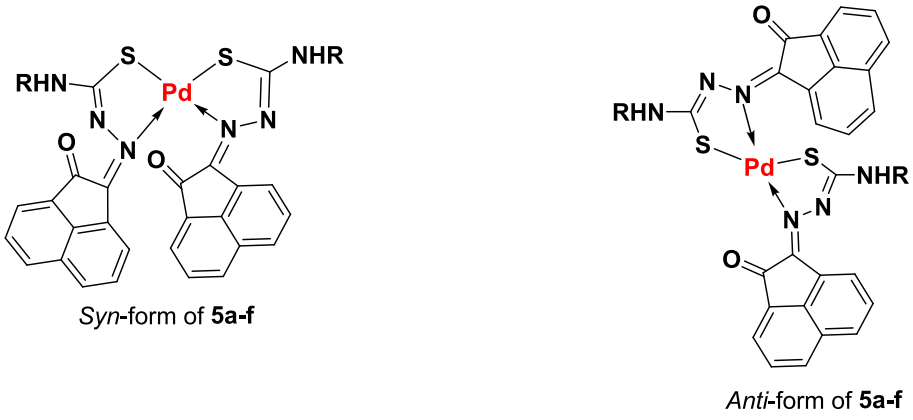

Fig. 7. *Syn*- and *anti*-structure of complexes 5a-f.

Table 5
MIC values (μg/ml) of compounds **5a-f** and **7a-f.**

Compd.	*B. subtilis*	*S. aureus*	*E. coli*	*K. pneumoniae*	*C. albicans*	*A. niger*
5a	0.066	0.066	0.033	0.033	0.033	0.066
5b	0.072	0.033	0.063	0.036	0.036	0.072
5c	0.070	0.035	0.070	0.035	0.035	0.070
5d	0.057	0.029	0.057	0.029	0.029	0.057
5e	0.077	0.035	0.077	0.077	0.035	0.070
5f	0.039	0.019	0.039	0.019	0.039	0.078
7a	0.061	0.030	0.030	0.030	0.030	0.061
7b	0.067	0.034	0.067	0.033	0.033	0.135
7c	0.061	0.030	0.031	0.061	0.018	0.018
7d	0.028	0.057	0.028	0.028	0.057	0.028
7e	0.082	0.045	0.041	0.041	0.041	0.020
7f	**0.066**	**0.018**	**0.018**	**0.033**	**0.027**	0.033
Ciprofloxacin	**0.018**	**0.018**	**0.018**	**0.018**	–	–
Fluconazole	–	–	–	–	0.020	0.020

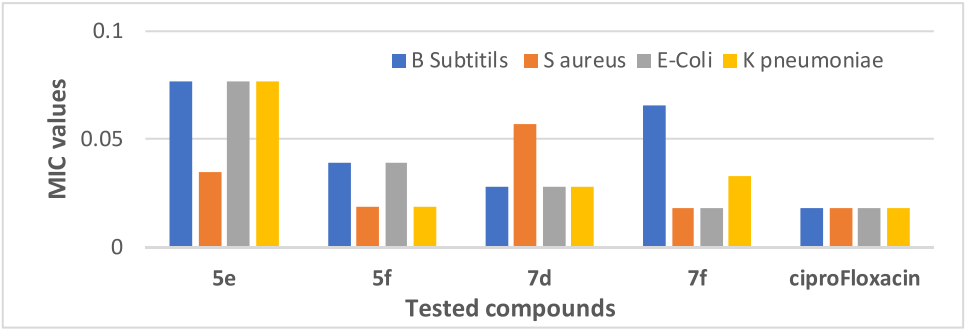

Fig. 8. Antibacterial activity of 5e, 5f, 7d, and 7f.

0.018 μg/mL, respectively, while **ciprofloxacin** has the same value of 0.018 μg/mL against both strains. Compound **7a** (R = Me) was 1.6-fold less potent than **7c** (R = cyclohexyl), with MIC values of 0.030 and 0.030 μg/mL against *S. aureus* and *E. coli*, respectively. Accordingly, the *m*-OMe substituent is important for antibacterial activity. It should also be noted that most of the compounds tested had only weak inhibitory activity against *B. subtilis*, a Gram-positive organism.

3.2.2. *Antifungal activity*

Compounds **5d**, **5e**, **7c**, and **7f** demonstrated promising antifungal activity against *C. albicans* with MIC values of 0.029, 0.023, 0.018, and 0.027 μg/ml, respectively, when compared to the reference **fluconazole**, which had a MIC value of 0.020 μg/ml (Fig. 9). Compound **7c** (R = cyclohexyl) outperformed **fluconazole** against *C. albicans*. In contrast, compound **7f** (R = R = 3-Ome-Ph) was 1.5-fold less potent, demonstrating that the cyclohexyl group was more tolerated than 3-OMe-Ph moiety for antifungal activity. Finally, compounds **5e** (R = phenyl) and **7c** (R = cyclohexyl) demonstrated potent antifungal activity against *A. Niger* with MIC values of 0.019 and 0.018 μg/ml, respectively, when compared to the reference **fluconazole**, which had a MIC value of 0.020 μg/ml. In contrast, the remaining compounds showed weak to good inhibitory activity.

3.2.3. *E. Coli DNA gyrase and topoisomerase IV inhibitory assay*

E. coli DNA gyrase and topoisomerase IV assays [49,50] were used to assess the inhibitory potency of the most active antibacterial derivatives **5e**, **5f**, **7d**, and **7f** against these two enzymes as potential targets for their antibacterial activity and the results are shown in Table 6. The results are presented as residual activities (Ras) of the enzyme at 1 μM of compounds or IC_{50} values for compounds with a RA of 50 % or lower. The compounds tested showed weak to moderate inhibition of *E. coli* DNA gyrase. Compounds **7d** and **7f** were found to be the most active, with inhibitory activities of *E. coli* DNA gyrase (IC_{50} = 297 ± 20 nM and 210 ± 15 nM, respectively) being 1.75 and 1.2-folds less potent than the

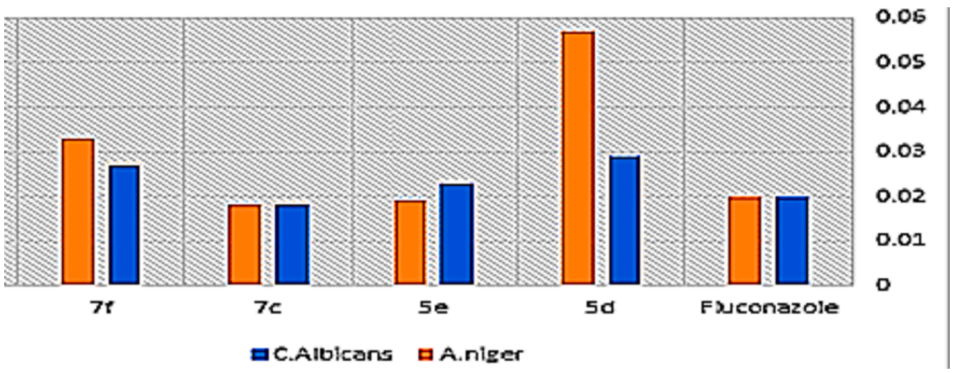

Fig. 9. Antifungal activity of compounds 5d, 5e, 7c, and 7f.

Table 6
Inhibitory activities of compounds **5e**, **5f**, **7d**, **7f**, and **Novobiocin** against *E. coli* DNA gyrase and topoisomerase IV.

Compound	IC_{50} (nM)[a] or RA (%) [b]	IC_{50} (μM)[a] or RA (%) [b]
	E. Coli DNA gyrase	*E. coli* topo IV
5e	73 %	87 %
5f	55 %	53 %
7d	297 ± 20 nM	21.50 ± 2.00 μM
7f	210 ± 15 nM	16.80 ± 1.50 μM
Novobiocin	170 ± 20 nM	11 ± 2 μM

[a] Concentration of compound that inhibits the enzyme activity by 50%.
[b] Residual activity of the enzyme at 1 μM of the compound.

reference **novobiocin** (IC_{50} = 170 ± 20 nM).

Compounds **5e**, **5f, 7d,** and **7f** were tested *in vitro* against *E. coli* topoisomerase IV. Compounds **7d** and **7f** showed promising results against topoisomerase IV (Table 6). Compounds **7d** and **7f** had IC_{50} values of 21.50 ± 2.00 μM and 16.80 ± 1.50 μM, respectively), and were also less potent than novobiocin (IC_{50} = 11 μM). Based on these findings, DNA gyrase and topoisomerase IV may be potential targets for the antibacterial activity of the new compounds, which require further optimization for more potent compounds.

4. Conclusion

The synthesis of Pd(II) and Ag(I) complexes of thiosemicarbazone by acenaphthenequinone was here reported. Bis(bidentate) complexes of both metals were obtained depending on the molar ratios of the ligands and the metal salts. Pd-complexes were formed *via* elimination of two moles of HCl during complexation between two moles of ligands and one mole of $PdCl_2$. However, one mole of $AgNO_3$ salt formed direct complexation with two moles of thiosemicarbazones to the corresponding cationic-anionic salts. The structure and geometry of the formed metal complexes were elucidated by IR, NMR, and UV–vis spectra. Elemental analysis and mass spectroscopy indicated the chemical formulae of the metal complexes. Molar conductance remarked the cationic-anionic character of silver complexes. DFT and TD-DFT calculations demonstrated the optimized molecular structures along with the UV–visible spectra of the Pd(II) and Ag(I) complexes (**5e** and **7e**, respectively). Antibacterial and antifungal activities of the obtained metal complexes were also investigated. Four metal complexes were found to be the most active and effective against the four bacterial strains. One of the Ag-thiosemicarbazone complexes (R = 3-OMe-Ph) showed MIC values of 0.066, 0.018, 0.018, and 0.033 μg/mL against *B. subtilis, S. aureus*, *E. coli,* and *K. pneumoniae*, respectively. Another four metal complexes containing Pd- and Ag complexes demonstrated promising antifungal activity against *C. albicans* with MIC values of 0.029, 0.023, 0.018, and 0.027 μg/ml, respectively, when compared to the reference **fluconazole**, which had a MIC value of 0.020 μg/ml. One of them revealed inhibitory activity of *E. coli* DNA gyrase (IC_{50} = 210 ± 15 nM, respectively) being 1.2-folds less potent than the reference **novobiocin** (IC_{50} = 170 ± 20 nM). The obtainable Pd- and Ag complexes would provide us an indication that they would become promising antimicrobial agents.

CRediT authorship contribution statement

Ashraf A. Aly: Conceptualization, Supervision, Writing, Editing. **Elham M. Abdallah** Conceptualization, Supervision. **Salwa A. Ahmed:** Conceptualization, Supervision. **Mai M. Rabee:** Methodology, Writing draft. **Olaf Fuhr:** X-ray, Editing. **Mahmoud A. A. Ibrahim:** DFT calculations and Revision. **Hayat Ali Alzahrani:** Biology, Writing, Revision. **Bahaa G.M. Youssif:** Biology, Writing, Revision

Declaration of competing interest

The authors declare that they have no known competing financial interests or personal relationships that could have appeared to influence the work reported in this paper.

Data availability

Data will be made available on request.

Acknowledgments

Mahmoud A. A. Ibrahim thanks the Center for High-Performance Computing (CHPC, http://www.chpc.ac.za), Cape Town, South Africa, for providing computational resources.

Funding.

Not Applicable

References

[1] P. Chellan, K.M. Land, A. Shokar, A. Au, S.H. An, C.M. Clavel, P.J. Dyson, C. de Kock, P.J. Smith, K. Chibale, G.S. Smith, Organomet. 31 (16) (2012) 5791–5799.
[2] S.A. Khan, A.M. Asiri, K. Al-Amry, M.A. Malik, Synthesis, characterization, electrochemical studies, and in vitro antibacterial activity of novel thiosemicarbazone and its cu(ii), ni(ii), and co(ii) complexes, The Scien Tific World J. 2014 (2014) 1–9.
[3] L. Yang, H. Liu, D. Xia, S. Wang, Antioxidant properties of camphene-based thiosemicarbazones: experimental and theoretical evaluation, Molecules 25 (6) (2020) 1192.
[4] M. Muralisankar, J. Haribabu, N.S. Bhuvanesh, R. Karvembu, A. Sreekanth, Synthesis, X-ray crystal structure, DNA/protein binding, DNA cleavage and cytotoxicity studies of N(4) substituted thiosemicarbazone based cop per(II)/nickel (II) complexes, Inorg. Chim. Acta 449 (2016) 82–95.
[5] I.M. Kenawy, M.M. Hassanien, M.H. Abdel-Rhman, R.R. Zaki, H.S. Rashed, Synthesis and characteriza tion of Hg(II) and Cd(II) complexes derived from the novel acenaphthaquinone-4-phenyl thiosemicarbazone and its CPE application, Egypt. J. Basic and Appl. Sciences 3 (2016) 106–117.
[6] N. Abdolhi, M. Aghaei, A. Soltani, H. Mighani, E.A. Ghaemi, M.B. Javan, A. D. Khalaji, S. Sharbati, M. Shafipour, H. Balakheyli, Synthesis and antibacterial activities of novel hg(ii) and zn(ii) complexes of bis(thiosemicarbazone) acenaphthenequinone loaded to MWCNTs, J. Struct. Chem. 60 (2019) 845–853.
[7] A.P. da Silva, M.V. Martini, C.M. de Oliveira, S. Cunha, J.E. de Carvalho, A.L. Ruiz, C.C. da Silva, Antitumor activity of ( )-α-bisabolol-based thiosemicarbazones against human tumor cell lines, Eur. J. Med. Chem. 45 (2010) 2987–2993.
[8] J. Baruah, R. Gogoi, N. Gogoi, G.A. Borah, thiosemicarbazone–palladium(II)–imidazole complex as an efficient pre-catalyst for Suzuki-Miyaura cross-coupling reactions at room temperature in aqueous media, Trans. Metal Chem. 42 (2017) 683–692.
[9] G. Munikumari, R. Konakanchi, V.B. Nishtala, G. Ramesh, L.R. Kotha, K. Chandrasekhar, C. Ramachandraiah, Palladium(II) complexes of 5-substituted isatin thiosemicarbazones: synthesis, spectroscopic characterization, biological evaluation and in silico docking studies, Synth. Commun. 49 (2019) 146–158.
[10] E. Ramachandran, D.S. Raja, N.S. Bhuvanesh, K. Natarajan, Mixed ligand palladium(II) complexes of 6- methoxy-2-oxo-1,2-dihydroquinoline-3-carbaldehyde 4N-substituted thiosemicarbazones with triphenylphosphine co-ligand: synthesis, crystal structure and biological properties, Dalton Trans. 41 (2012) 13308–13323.
[11] P. Chung, Y. Huentupil, W. Rabanal, J. Cisterna, I. Brito, R. Arancibia, Synthesis, characterization, X-ray structure, electrochemistry, photocatalytic activity and DFT studies of heterotrinuclear Ni(II), Pd(II) and Zn(II) complexes containing a formylferrocene thiosemicarbazone ligand, Appl. Organomet. Chem. 34 (2020) e5974.
[12] A.D. Khalaji, E. Shahsavani, N. Feizi, M. Kucerakova, M. Dusek, R. Mazandarani, Silver(I) thiosemicarbazone complex [Ag(catsc)(PPh3)2]NO3: synthesis, characterization, crystal structure, and antibacterial study, Comptes Rendus Chim. 20 (2017) 534–539.
[13] D.E. Silva, A.B. Becceneri, M.C. Solcia, J.V. Santiago, M.B. Moreira, J.A.G. Neto, F. R. Pavan, M.R. Cominetti, J.C. Pereira, A.V. Netto, Cytotoxic and apoptotic effects of ternary silver(i) complexes bearing 2- formylpyridine thiosemicarbazones and 1,10-phenanthroline, Dalton Trans. 49 (2020) 5264–5275.
[14] T.S. Lobana, Activation of C-H bonds of thiosemicarbazones by transition metals: synthesis, structures and importance of cyclometallated compounds, RSC Adv. 5 (2015) 37231–37274.

[15] C.G. Oliveira, I. Romero-Canelón, J.P. Coverdale, P.I.S. Maia, G.J. Clarkson, V. M. Deflon, P.J. Sadler, Novel tetranuclear Pd^{II}_4 and Pt^{II}_4 anticancer complexes derived from pyrene thiosemicarbazones, Dalton Trans. 49 (2020) 9595–9604.

[16] E. Ramachandran, P. Kalaivani, R. Prabhakaran, M. Zeller, J.H. Bartlett, P. O. Adero, T.R. Wagner, K. Natarajan, Synthesis, characterization, crystal structure and DNA binding studies of Pd(II) complexes containing thiosemicarbazone and triphenylphosphine/triphenylarsine, Inorg. Chim. Acta 385 (2012) 94–99.

[17] A.A. Shoukry, M.S. Mohamed, DNA-binding, spectroscopic and antimicrobial studies of palladium(II) complexes containing 2,2′-bipyridine and 1-phenylpiperazine. Spectrochim. Acta Part A: Mol. & Biomol, Spectroscopy 96 (2012) 586–593.

[18] I. Kizilcikli, Y.D. Kurt, B. Akkurt, A.Y. Genel, S. Birteksöz, G. Ötük, B., Ülküseven Antimicrobial activity of a series of thiosemicarbazones and their ZnII and PdII complexes, Folia Microbiol. 52 (2007) 15–25.

[19] S.A. Khan, M. Yusuf, Synthesis, spectral studies and in vitro antibacterial activity of steroidal thiosemicarbazone and their palladium (Pd (II)) complexes, Eur. J. Med. Chem. 44 (5) (2009) 2270–2274.

[20] S. Medici, M. Peana, G. Crisponi, V.M. Nurchi, J.I. Lachowicz, M. Remelli, M. A. Zoroddu, Silver coordination compounds: A new horizon in medicine, Coord. Chem. Reviews 327 (2016) 349–359.

[21] S. Medici, M. Peana, V.M. Nurchi, M.A. Zoroddu, Medical Uses of Silver: History, Myths, and Scientific Evidence, J. Med. Chem. 62 (2019) 5923–5943.

[22] D.E. Silva, A.B. Becceneri, M.C. Solcia, J.V. Santiago, M.B. Moreira, J.A.G. Neto, F. R. Pavan, M.R. Cominetti, J.C. Pereira, A.V. Netto, Cytotoxic and apoptotic effects of ternary silver(I) complexes bearing 2-formylpyridine thiosemicarbazones and 1,10-phenanthroline, Dalton Trans. 49 (2020) 5264–5275.

[23] X. Liang, S. Luan, Z. Yin, M. He, C. He, L. Yin, Y. Zou, Z. Yuan, L. Li, X. Song, Recent advances in the medical use of silver complex, Eur. J. Med. Chem. 157 (2018) 62–80.

[24] A. Llie, IC. I. Rat, S. Scheutzow, C. Kiske, K. Lux, T. M. Klapötke, C. Silvestru, K. Karaghiosoff, Metallophilic Bonding and Agostic Interactions in Gold(I) and Silver (I) Complexes Bearing a Thiotetrazole Unit. Inorg. Chem. 50 (2011) 2675-2684.

[25] A. Castiñeiras, N. Fernández-Hermida, I. García-Santos, J.L. Pérez-Lustres, I. Rodríguez-González, Luminescent complexes of silver(I) with pyridylbis(3-hexamethyleneiminyl thiosemicarbazone): effect of the counterion on the nuclearity, Dalton Trans. 41 (2012) 3787–3796.

[26] R.B. Thurman, C.P. Gerba, The molecular mechanisms of copper and silver ion disinfection of bacteria and viruses, CRC Crit. Rev. Environ. Control 18 (1989) 295–315.

[27] R.M.E. Richards, H.A. Odelola, B. Anderson, Effect of silver on whole cells and spheroplasts of a silver resistant *Pseudomonas aeruginosa*, Microbios 39 (1984) 151–158.

[28] J.I. Manchester, D.D. Dussault, J.A. Rose, P.A. Boriack-Sjodin, M. Uria-Nickelsen, G. Ioannidis, S. Bist, P. Fleming, K.G. Hull, Discovery of a novel azaindole class of antibacterial agents targeting the ATPase domains of DNA gyrase and Topoisomerase IV, Bioorg. Med. Chem. Lett. 22 (2012) 5150–5156.

[29] C. Sissi, M. Palumbo, In front of and behind the replication fork: bacterial type IIA topoisomerases, Cell. Mol. Life Sci. 67 (2010) 2001–2024.

[30] A.A. Aly, E.M. Abdallah, S.A. Ahmed, A.K. Awad, M.M. Rabee, S.M. Mostafa, S. Bräse, Metal complexes of new thiocarbohydrazones of Cu(I), Co(II), and Ni(II); identification by NMR, IR, mass, UV spectra, and DFT calculations, J. Sulf. Chem. 44 (3) (2023) 282–303.

[31] A.A. Aly, S. Bräse, P. Weis, Tridentate and bidentate copper complexes of [2.2] paracyclophanyl-substituted thiosemicarbazones, thiocarbazones, hydrazones and thioureas, J. Mol. Stru. (2019, 1178,) 311–326.

[32] S. Kumar, A. Hansfa, A. Chandra, A. Kumar, M. Kumar, S. Sithambaresan, M. S. Haque, V. Kumar, R.P. John, Co(II), Ni(II), Cu(II) and Zn(II) complexes of acenaphthoquinone 3-(4-benzylpiperidyl)- thiosemicarbazone: Synthesis, structural, electrochemical and antibacterial studies, Polyhedron 134 (2017) 11–21.

[33] D.M. Campoli-Richards, J.P. Monk, A. Price, P. Benfield, P.A. Todd, A. Ward, Ciprofloxacin, A Review of Its Antibacterial Activity, Pharmacokinetic Properties and Therapeutic Use Drugs 35 (4) (1988) 373–447.

[34] P. T. McKeny, T. A. Nessel, P. M. Zito, Antifungal Antibiotics. StatPearls Publishing, Treasure Island (FL), United States. Copyright © 2023. Bookshelf ID: NBK538168PMID: 30844195.

[35] B. Lanoot, M. Vancanneyt, I. Cleenwerck, L. Wang, W. Li, Z. Liu, J. Swings, The search for synonyms among streptomycetes by using SDS-PAGE of whole-cell proteins. Emendation of the species *Streptomyces aurantiacus*, *Streptomyces cacaoi subsp. cacaoi*, *Streptomyces caeruleus* and *Streptomyces violaceus*, Internat. J. Syst. & Evol. Microbiol. 52 (3) (2002) 823–829.

[36] A.A. Aly, N.K. Mohamed, A.A. Hassan, K.M. El-Shaieb, M.M. Makhlouf, S. Bräse, M. Nieger, A.B. Brown, Functionalized 1,3-Thiazolidin-4-Ones from 2-Oxo-Acenaphthoquinylidene- and [2.2]Paracyclophanylidene- Thiosemicarbazones, Molecules 24 (2019) 3069.

[37] S. L. Pascu, P. A. Waghorn, B. W. Kennedy, R. L. Arrowsmith, S. R. Bayly, J. R. Dilworth, M. Christlieb, R. M. Tyrrell, J. Zhong, R. M. Kowalczyk, Fluorescent Copper(II) Bis(thiosemicarbazonates): Synthesis, Structures, Electron Paramagnetic Resonance, Radiolabeling, *In Vitro* Cytotoxicity and Confocal Fluorescence Microscopy Studies. Chem.–An Asian J. 5(3) (2010) 506-519.

[38] A. H. Mohamed, M. B. Alshammari, A. A. Aly, K. U. Sadek, A. Ahmad, E. A. Aziz, A. F. El-Yazbi, E. J. El-Agroudy, M. E. Abdelaziz, New imidazole-2-thiones derived by acenaphythylenone as dual DNA intercalators and topoisomerase II inhibitors: structural optimization, molecular modeling and apoptosis studies. J. Enzyme Inhib. & Med. Chem. 2024 (under publication).

[39] H.A. Hofny, M.F. Mohamed, H.A. Gomaa, S.A. Abdel-Aziz, B.G.M. Youssif, N.A. El-Koussi, A.S. Aboraia, Design, synthesis, and antibacterial evaluation of new quinoline-1,3,4-oxadiazole and quinoline-1,2,4- triazole hybrids as potential inhibitors of DNA gyrase and topoisomerase IV, Bioorg. Chem. 112 (2021) 104920.

[40] L. H. Al-Wahaibi, A. A. Amer, A. A. Marzouk, H. A. M. Gomaa, B. G. M. Youssif, A. A. Abdelhamid, Design, Synthesis, and Antibacterial Screening of Some Novel Heteroaryl-Based Ciprofloxacin Derivatives as DNA Gyrase and Topoisomerase IV Inhibitors Pharmaceuticals 14(5) (2021), 399.

[41] O.V. Dolomanov, L.J. Bourhis, R.J. Gildea, J.A.K. Howard, H. Puschmann, *OLEX2*: a complete structure solution, refinement and analysis program, J. Appl. Cryst. 42 (2009) 339–341.

[42] G.M. Sheldrick, SHELXT - Integrated space-group and crystal-structure determination, Acta Cryst 71A (2015) 3–8.

[43] G.M. Sheldrick, Crystal structure refinement with SHELXL, Acta Cryst C 71 (2015) 3–8.

[44] J. Frisch, G.W.T., H. B. Schlegel, G. E. Scuseria, M. A. Robb, J. R. Cheeseman, G. Scalmani, V. Barone, B. Mennucci, G. A. Petersson, H. Nakatsuji, M. Caricato, X. Li, H. P. Hratchian, A. F. Izmaylov, J. Bloino, G. Zheng, J. L. Sonnenberg, M. Hada, M. Ehara, K. Toyota, R. Fukuda, J. Hasegawa, M. Ishida, T. Nakajima, Y. Honda, O. Kitao, H. Nakai, T. Vreven, J. A. Montgomery, Jr., J. E. Peralta, F. Ogliaro, M. Bearpark, J. J. Heyd, E. Brothers, K. N. Kudin, V. N. Staroverov, R. Kobayashi, J. Normand, K. Raghavachari, A. Rendell, J. C. Burant, S. S. Iyengar, J. Tomasi, M. Cossi, N. Rega, J. M. Millam, M. Klene, J. E. Knox, J. B. Cross, V. Bakken, C. Adamo, J. Jaramillo, R. Gomperts, R. E. Stratmann, O. Yazyev, A. J. Austin, R. Cammi, C. Pomelli, J. W. Ochterski, R. L. Martin, K. Morokuma, V. G. Zakrzewski, G. A. Voth, P. Salvador, J. J. Dannenberg, S. Dapprich, A. D. Daniels, Ö. Farkas, J. B. Foresman, J. V. Ortiz, J. Cioslowski, and D. J. Fox, Gaussian, Inc., Wallingford CT, Gaussian 09, Revision E.01. 2009.

[45] W.J. Geary, The use of conductivity measurements in organic solvents for the characterisation of coordination compounds, Coord. Chem. Reviews 7 (1971) 81–122.

[46] N. Bharti, S. Sharma, F. Naqvi, A. Azam, New palladium(II) complexes of 5-nitro-thiophene-2-carboxaldehyde thiosemicarbazones: synthesis, spectral studies and In vitro anti-Amoebic activity, Bioorg. & Med. Chem. 11 (11) (2003) 2923–2929.

[47] P. Sharma, H. Nath, A. Frontera, M. Barcelo-Oliver, A.K. Verma, S. Hussain, M. K. Bhattacharyya, Biologically relevant unusual cooperative assemblies and fascinating infinite crown-like supramolecular nitrate–water hosts involving guest complex cations in bipyridine and phenanthroline- based Cu(II) coordination compounds: antiproliferative evaluation and theoretical studies, New J. Chem. 45 (2021) 8269–8282.

[48] H. Djouama, et al., Geometry optimization and UV/Vis spectra of organometallic chalcones functionalized with a benzo-15-crown-5 fragment: A DFT/TD-DFT investigation, Inorganica Chim. Acta. 561 (2024) 121866.

[49] F.O.A. Firas, Y. Cao, H. Zhai, S.A. Abdel-Aziz, H.A.M. Gomaa, B.G.M. Youssif, C. Wu, Novel 1,2,4- oxadiazole/pyrrolidine hybrids as DNA gyrase and topoisomerase IV inhibitors with potential antibacterial activity, Arab. J. Chem. 15 (2022) 103538.

[50] F.O.A. Firas, Y. Cao, L. Wang, H. Zhai, A.H. Abdelazeem, H.A.M. Gomaa, B.G. M. Youssif, C. Wu, New 1,2,4-oxadiazole/pyrrolidine hybrids as topoisomerase IV and DNA gyrase inhibitors with promising antibacterial activity, Archiv Der Pharm. (2022) e2100516.